COPY RIGHT

Title:- **A NOVEL ISOLATED DC-DC CONVERTER FOR HIGH STEP-UP RATIO FOR GRID CONNECTED APPLICATIONS**

Paper Authors
[1]Yenumula Vyshnavi,[2]Ulisi Ganesh

Editor IJIEMR

www.ijiemr.com

To Secure Your Paper As Per UGC Guidelines We Are Providing A Electronic Bar Code

A NOVEL ISOLATED DC-DC CONVERTER FOR HIGH STEP-UP RATIO FOR GRID CONNECTED APPLICATIONS

[1]Yenumula Vyshnavi,[2]Ulisi Ganesh

[1]M-tech ,student Scholar,Department of Electrical & Electronics Engineering,Velaga Nageswara Rao College of Engineering, Ponnuru; Guntur (Dt); A.P, India.

[2]M-Tech,Assistant ProfessorDepartment of Electrical & Electronics Engineering,Velaga Nageswara Rao College Of Engineering, Ponnuru;Guntur (Dt); A.P

Abstract- This paper focuses on the design of an isolated dc–dc converter for railway applications and the requirements for the investigated DC-DC converter. First of all the voltage should be stepped up to sufficient level at which the DC/AC conversion can be performed to AC mains voltage requirements. Overall performance of the renewable energy system is then affected by the efficiency of step-up DC/DC converters, which are the key parts in the system power chain. This review is focused on high efficiency step-up DC/DC converters with high voltage gain.

Although DC/DC-converters exist without input-output isolation, most DC/DC-converters use an internal transformer and the output is electrically (galvanically) isolated from the input. The basic input to output isolation can be used to provide either a simple isolated output power source, A high step-up converter adopts boost converter with interleaved mode and a coupled inductor to increase its step-up voltage ratio. The interleaving technique connects the converter in parallel to share the power flow, this reduce the size, weight, and volume of the inductors and capacitors. Without using of high duty ratio this converter achieves a high step-up voltage-conversion ratio through a coupled inductor and the converter. The proposed concept can be implemented to isolated DC-DC converter high step up ratio gain for grid connected applications by using MATLAB/SIMULINK software.

Index Terms—DC–DC power conversion, power electronics, power supplies, rail transportation electronics.

I. INTRODUCTION

Solar energy is the most low cost, competition free, universal source of energy as sun shines throughout. This energy can be converted into useful electrical energy using photovoltaic technology. The steady state reduction of price per peak watt and simplicity with which the installed power can be increased by adding panels are attractive features of PV technology. Among the many applications of PV energy, pumping is the most promising. In a PV pump storage system, solar energy is stored, when sunlight is available as potential energy in water reservoir and consumed according to demand. There are advantages in avoiding the use of large banks of lead acid batteries, which are heavy and expensive and have one fifth of the lifetime of a PV panel. A number of simulation DC motor driven PV pumps are already in use in several parts of the world, but they suffer from maintenance problems due to the presence of the commutator and brushes. Hence a pumping system based on an induction motor can be an attractive proposal where reliability and maintenance-free operations with less cost are important. The effective operation of Induction motor is based on the choice of suitable converter-inverter system that is fed to Induction Motor.

For PV applications like pumping these converters could do a good job as pumping is carried out at high power. Thus a new push pull converter which is two switch topology can do justice by giving a high power throughout. The Induction Motors are the AC motors and hence from converter, an inverter system is also

required to obtain an AC voltage. This inverter is chosen based on its advantages and it is fed to induction motor.

Photovoltaic technology is one of the most promising for distributed low-power electrical generation. The steady reduction of price per peak watt over recent years and the simplicity with which the installed power can be increased by adding panels are some of its attractive features. Among the many applications of photovoltaic energy, pumping is one of the most promising. In a photovoltaic pump-storage system, solar energy is stored, when sunlight is available, as potential energy in a water reservoir and then consumed according to demand. There are advantages in avoiding the use of large banks of lead-acid batteries, which are heavy and expensive and have one-fifth of the lifetime of a photovoltaic panel. It is important, however, that the absence of batteries does not compromise the efficiency of the end-to-end power conversion chain, from panels to mechanical pump. Photovoltaic panels require specific control techniques to ensure operation at their maximum power point (MPP). Impedance matching issues mean that photovoltaic arrays may operate more or less efficiently, depending on their series/parallel configuration.

II. TOPOLOGY OVERVIEW

The field of high-power-density dc–dc converters has beenaddressed often in the last decades. From the beginning,the conventional full-bridge converter topology has been thepreferred choice to realize a high-power dc–dc converter [1].However, due to problems with the leakage inductance of thetransformer and, consequently, reverse recovery losses of theoutput diodes, the maximum switching frequency is limited.To solve this problem,

several solutions were presented,including active clamps and/or auxiliary circuits [2]–[4]. Thesesolutions enable higher switching frequencies at the expense ofadditional components and could lead to higher device stress.The additional components impede the increase in powerdensity and increased complexity, while the efficiency is oftennot better compared to other zero-voltage switching (ZVS) andzero-current switching (ZCS) techniques.Resonant converter topologies offer possibilities for ZVS orZCS, enabling high efficiencies and power densities [5]–[7]. Theseries resonant or LLC converter provides a load independentoperating point with unity voltage gain at a switching frequencynear the resonance frequency [6], [8]–[10]. However, this loadindependent operating point is lost when the input and/or outputvoltage changes, and switching frequency control is necessary toregulate the output voltage. Therefore, a boost converter can beused to regulate the input voltage in order to guarantee operationin the load independent operating point [10], [11]. Alternatively,the resonance circuit can be influenced by a switch-controlledcapacitor, resulting in fixed frequency operation [12]. Despitethe provided solutions, the LLC converter still suffers from highrms phase currents, requiring a relatively large series resonantcapacitor that leads to a decreased power density. The additionalboost converter or switch-controlled capacitor also deterioratesthe power density and efficiency.

The dual active bridge (DAB) topology introduced in [1]is an attractive alternative to the problems with the classicalfull-bridge topology. In comparison with the conventional fullbridge topology, the output inductor is transferred to the ac side,and is in series with the leakage inductance. Consequently, theenergy in

the leakage inductance is transferred to the load without causing reverse recovery losses in the output diodes. Thisallows higher switching frequencies and, therefore, an increasein power density. Furthermore, the use of an active output bridgealso increases the power density of the transformer [1]. Whenthe desired inductance can be incorporated in the transformer,again the power density can be increased. In [13], very highpower densities, up to 11.13kW/L, are reported.A three-phase DAB, also proposed in [1], has some advantages in comparison to the single-phase DAB. The three-phaseDAB has lower turn-off currents in the switches and lowerrms currents per phase. Also, the VA ratings for the input andoutput filters are significantly lower and can even go to zerodue to the three-phase characteristics. Besides the lower VAratings, the effective ripple frequency of the filter currents isthree times higher, allowing to use smaller filters. Comparedto the single-phase DAB, the currents through the transformerwindings are much more sinusoidal, resulting in reduced highfrequency losses in the transformers [14]. A comprehensivecomparison of single-phase and three-phase DAB topologies isgiven in [1].Both the single-phase and three-phase DAB topologies sufferfrom a limited soft-switching range in case the input voltage andthe reflected output voltage are not equal. For the single-phaseDAB, there exist switching strategies or modulation schemes forincreasing the soft-switching range. These are described. Here, the soft-switching operating range is increased andalso the overall efficiency can be increased with a minimum lossmodulation strategy. The three-phase DAB does notpossess these advantageous switching possibilities. The phaseshift angle φ between the bridge voltage is the only controlvariable as the symmetrical properties of the three-phase systemhave to be maintained [14].Although the three-phase DAB has less switching possibilities, compared to the single-phase DAB, and includes fourextra switches, the topology has the most preferred propertiesfor designing a high-power density isolated dc–dc converter. Ithas the lowest component ratings and is capable of achievinghigher output powers with possibly the highest power density.For APU applications in light rail vehicles, high-power capability and power density are decisive. Therefore, the three phaseDAB topology is selected in this study.

III. THREE-PHASE DAB DC–DC CONVERTER

The three-phase DAB, shown in Fig. 1(a), consists of twothree-phase bridges coupled with a three-phase transformer connected in Y–Y. The bridges are operated in six-step mode at aconstant frequency. By applying a phase shift between the inputand Output Bridge, the power flow can be controlled. Becausethe converter is symmetrical from input to output, bidirectionalpower flow is possible. The transformer leakage inductances areused as current transfer elements and, therefore, not consideredas parasitic. If the magnetizing inductance Lm is neglected, anequivalent circuit can be used for analysis. In this circuit, onlythe total leakage inductance Ls seen from the primary side isconnected between the phase legs from the input and outputbridge. The corresponding idealized waveforms are shown inFig. 1(b).

A. Analysis

To analyze the soft-switching region, the current of phase Ais defined for the first six intervals as depicted in Fig. 1(b). Thecurrent iA in the different intervals is given in (3) for phaseshifts of $0 \leq \varphi \leq \pi 3$. For phase shifts of $\pi 3 \leq \varphi \leq 23\pi$, a secondset of equations, not given here, is

utilized for further analysisof the soft-switching region. The magnetizing inductance Lmof the transformer is neglected in the analysis.Furthermore, the angular frequency is defined as ω = 2πfs,with fs the switching frequency in Hertz. The transformer'sleakage inductance is indicated with Ls and the input and outputvoltage are defined as Vi and Vo, respectively. The reflected output voltage is given by Vo= VoN, with N the turns ratio ofthe transformer.Because the phase current is symmetric, the current iA(0) canbe found by solving the set of equations, assuming steady-state

Fig.1. Three-phase DAB. (a) Topology. (b) Idealized waveforms, gatingsignals can be found in [1].

Condition iA(0) = −iA(π). This results in

$$i_A(0) = \frac{1}{3\omega L_s}\left[\frac{2\pi}{3}(V_o' - V_i) - V_o'\phi\right] \quad (1)$$

B. Output Power
Under the assumption of a lossless converter, the output powerPocan be found with

$$P_o = P_i = \frac{3}{\pi}\int_0^\pi v_{AP}(\theta)i_A(\theta)d\theta \quad (2)$$

$$i_A(\theta) = \begin{cases} i_A(0) + \frac{V_i + V_o'}{3\omega L_s}\theta & \forall\ 0 \le \theta \le \phi & \text{:interval 1} \\ i_A(\phi) + \frac{V_i - V_o'}{3\omega L_s}(\theta - \phi) & \forall\ \phi \le \theta \le \frac{\pi}{3} & \text{:interval 2} \\ i_A(\frac{\pi}{3}) + \frac{2V_i - V_o'}{3\omega L_s}(\theta - \frac{\pi}{3}) & \forall\ \frac{\pi}{3} \le \theta \le \frac{\pi}{3} + \phi & \text{:interval 3} \\ i_A(\frac{\pi}{3} + \phi) + \frac{2V_i - 2V_o'}{3\omega L_s}(\theta - \frac{\pi}{3} - \phi) & \forall\ \frac{\pi}{3} + \phi \le \theta \le \frac{2\pi}{3} & \text{:interval 4} \\ i_A(\frac{2\pi}{3}) + \frac{V_i - 2V_o'}{3\omega L_s}(\theta - \frac{2\pi}{3}) & \forall\ \frac{2\pi}{3} \le \theta \le \frac{2\pi}{3} + \phi & \text{:interval 5} \\ i_A(\frac{2\pi}{3} + \phi) + \frac{V_i - V_o'}{3\omega L_s}(\theta - \frac{2\pi}{3} - \phi) & \forall\ \frac{2\pi}{3} + \phi \le \theta \le \pi & \text{:interval 6} \end{cases} \quad (3)$$

Finally, the expression of the output power for $0 \le \varphi \le \frac{2}{3}\pi$ is

$$P_o = \begin{cases} \frac{V_i V_o'}{\omega L_s}\phi\left[\frac{2}{3} - \frac{\phi}{2\pi}\right] & \text{for } 0 \le \phi \le \frac{\pi}{3} \\ \frac{V_i V_o'}{\omega L_s}\left[\phi - \frac{\phi^2}{\pi} - \frac{\pi}{18}\right] & \text{for } \frac{\pi}{3} \le \phi \le \frac{2\pi}{3} \end{cases} \quad (4)$$

C. Soft-Switching Region
Minimizing the switching losses is the key to achieve a highswitching frequency. The turn-on losses are of main interestbecause excessive losses in the switch and the antiparallel diodecan arise when the antiparallel diodes experience the reverserecovery process. The input bridge faces this problem wheniA(0) > 0. Therefore, the current has to fulfill iA(0) ≤ 0 toensure soft-switching in the input bridge. During the switchingtransient, the current iA is considered constant. Rewriting (1)to the required constraint gives the phase shift for ensuring softturn-on of the switches in the input bridge, this is found to be

$$\phi_i \ge \frac{2\pi(V_o' - V_i)}{3V_o'} \quad (5)$$

A similar derivation can be made for the output bridge, wherethe output bridge is soft-switching for iA(φ) ≥ 0. Using (3) and(1) gives the
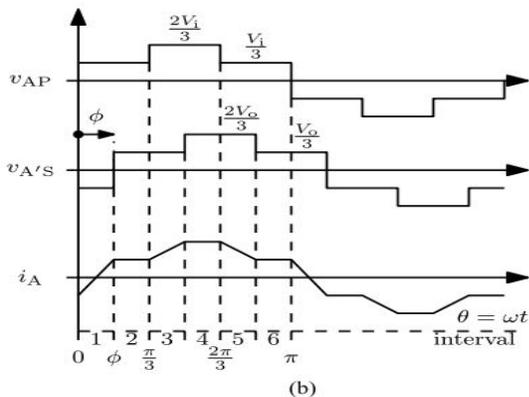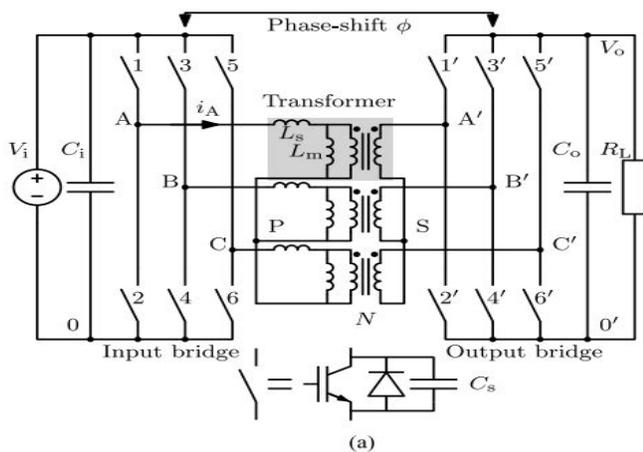
required phase shift to ensure soft turn-on of theswitches in the output bridge, resulting in

$$\phi_o \geq \frac{2\pi(V_i - V_o')}{3V_i} \quad (6)$$

1) Impact of ZVS Capacitors: ZVS capacitors, or snubbercapacitors, are used to reduce turn-off losses. These are connected in parallel to the switches and supplement the output capacitance, as can be seen in Fig. 1(a). After a switch turns OFF,there is a small blanking time tb before the opposite switch ofthe same leg turns on. During tb, the current commutates to theZVS capacitors and divides equally over the two capacitors ofthe phase leg. In this transition, one capacitor is charged whilethe other is discharged. This implies that the load current must behigh enough to enable a full charge or discharge of the ZVS capacitors for a given tb. Assuming a constant current during theswitching transient, the soft-switching constraint for enablingsoft turn-on of the switches in the input bridge is changed to

$$i_A(0) + \frac{2C_s V_i}{t_b} \leq 0 \quad (7)$$

and for the output bridge to

$$i_A(\phi) - \frac{2C_s V_o}{t_b N} \geq 0 \quad (8)$$

Where Cs represents a ZVS capacitor connected in parallel tothe switch, and tb is a fixed blanking time. A more accurate, current depending charge-based ZVS analysis is reported.However, to investigate the impact of the ZVS capacitors andapproximate the soft-switching region, the presented currentbased method is sufficient.Solving (7) and (8) for the phase-shift φ gives the softswitching region for

the input bridge and the output bridge,respectively. These are given by

$$\phi_i \geq \frac{2\pi_i(V_o' - V_i)}{3V_o'} + \frac{2C_s V_i}{V_o' t_b} 3\omega L_s \quad (9)$$

$$\phi_o \geq \frac{2\pi(V_i - V_o')}{3V_i} + \frac{2C_s V_o}{V_i t_b N} 3\omega L_s \quad (10)$$

D. Extension of the Soft-Switching Region

Auxiliary power converters for railway applications have tobe able to operate from no-load to full-load conditions overthe whole input voltage range. This means that the converterhas to operate outside the soft-switching region. Therefore, twomethods to extend the soft-switching operation of the converterhave been investigated.

1) Auxiliary Inductors: The first method is based on addingreactive currents to fully charge or discharge the ZVS capacitorsduring the switching transient. The reactive currents are injectedwith three star-connected auxiliary inductors per bridge. This has the same effect as the magnetizinginductances of the transformers, which are also connected instar. However, separate auxiliary inductors are preferred tohave more design flexibility.The peak current, injected by the auxiliary inductors duringthe switching transient, is calculated from the voltage waveforms shown in Fig. 1(b). For the input bridge, the peak currentis calculated as

$$\hat{i}_{a-i} = \frac{2\pi V_i}{9\omega L_{a-i}} \quad (11)$$

and for the output bridge as

$$\hat{i}_{a-o} = \frac{2\pi V_o}{9\omega L_{a-o} N} \quad (12)$$

Next, the soft-switching constraints from (7) and (8) can beextended to

$$i_A(0) + \frac{2C_s V_i}{t_b} - \frac{2\pi V_i}{9\omega L_{a-i}} \leq 0 \qquad (13)$$

and for the output bridge to

$$i_A(\phi) - \frac{2C_s V_o}{t_b N} + \frac{2\pi V_o}{9\omega L_{a-o} N} \geq 0 \qquad (14)$$

Then, the soft-switching region can be calculated with the minimum phase shift for the input bridge

$$\phi_i \geq \frac{2\pi(V_o' - V_i)}{3V_o'} + \frac{2C_s V_i}{V_o' t_b} 3\omega L_s - \frac{2\pi V_i L_s}{3V_o' L_{a-i}} \qquad (15)$$

and for the output bridge

$$\phi_o \geq \frac{2\pi(V_i - V_o')}{3V_i} + \frac{2C_s V_o}{V_i t_b N} 3\omega L_s - \frac{2\pi V_o L_s}{3V_i L_{a-o} N} \qquad (16)$$

As shown with (15) and (16), the auxiliary inductance decreases the required phase-shift for operating in a soft-switchingmanner. To achieve soft-switching in the whole operating range,(15) and (16) should be solved for zero phase-shift, i.e., no-loadcondition. The corresponding values. Forrelatively low- and high-input voltages, the required values forLa−i and La−o are low and, therefore, also causing high reactive currents. The use of auxiliary inductors presents a cleardisadvantage due to the reduced efficiency and power density.

2) Burst Mode: The second method does not use any extracomponents but relies on a straightforward switching strategy.When the required output power Po is lower than the minimumload for soft switching, the converter switches from continuousmode to burst mode. In the burst mode, the converter operateswith an output power Pb high enough to enable soft-switching.An example of the burst mode with the corresponding waveforms is shown in Fig. 2(a). The average output power is definedas

$$<p_o> = \frac{n}{m} P_b, \qquad \forall \quad 1 \leq n \leq m \qquad (17)$$

Where n is the amount of switching cycles operating with po =Pb and m is the total amount of switching cycles of one burstcycle. The value of Pb depends on the soft-switching region ofthe converter.When nTs < t ≤ mTs, the output power po = 0 W, thus theoutput capacitor delivers the required current to the load, introducing a small voltage ripple. The output voltage ripple can becalculated with

$$\Delta v_o = \frac{I_o \Delta t}{C_o} \qquad (18)$$

Where Io =<po >Vo=nPbmVoand Δt = m−nfs . This results in

$$\Delta v_o = \frac{n(m-n)P_b}{m V_o C_o f_s} \qquad (19)$$

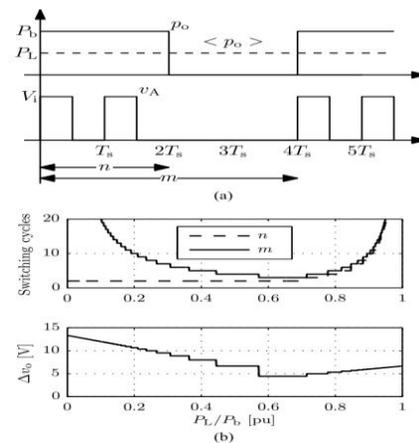An example of the output voltage ripple with n ≥ 2 is shownin Fig. 2(b).

Fig. 2. Burst-mode waveforms. (a) Burst-mode definitions. (b) Output voltageripple with n ≥ 2, Pb = 80 kW, Vo = 600 V, Co = 1 mF, and fs = 20 kHz.

The downside of this method is the need for a larger outputcapacitance for the same voltage ripple requirements in normal operation without the burst mode. Furthermore, while

International Journal for Innovative Engineering and Management Research
A Peer Reviewed Open Access International Journal
www.ijiemr.com

theswitching frequency is unchanged, the converter becomes audible due to the discontinuous operation.

IV. A PHOTOVOLTAIC SYSTEM

A photovoltaic system, converts the light received from the sun into electric energy. In this system, semi conductive materials are used in the construction of solar cells, which transform the self contained energy of photons into electricity, when they are exposed to sun light. The cells are placed in an array that is either fixed or moving to keep tracking the sun in order to generate the maximum power [9]. These systems are environmental friendly without any kind of emission, easy to use, with simple designs and it does not require any other fuel than solar light. On the other hand, they need large spaces and the initial cost is high.

PV array are formed by combine no of solar cell in series and in parallel. A simple solar cell equivalent circuit model is shown in figure. To enhance the performance or rating no of cell are combine. Solar cell are connected in series to provide greater output voltage and combined in parallel to increase the current. Hence a particular PV array is the combination of several PV module connected in series and parallel. A module is the combination of no of solar cells connected in series and parallel.

The photovoltaic system converts sunlight directly to electricity without having any disastrous effect on our environment. The basic segment of PV array is PV cell, which is just a simple p-n junction device. The fig.1.4 manifests the equivalent circuit of PV cell. Equivalent circuit has a current source (photocurrent), a diode parallel to it, a resistor in series describing an internal resistance to the flow of current and a shunt resistance which expresses a leakage current. The current supplied to the load can be given as.
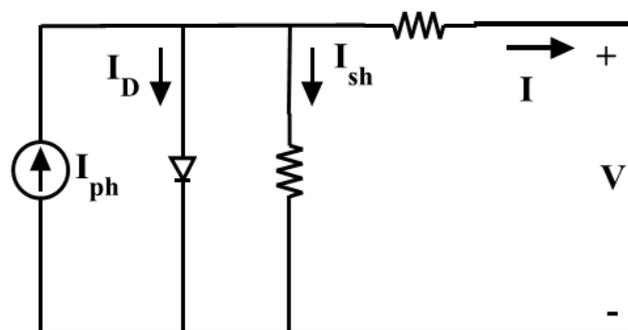
Equivalent circuit of Single diode modal of a solar cell

$$I = I_{PV} - I_O\left[\exp\left(\frac{V + IR_S}{aV_T}\right) - 1\right] - \left(\frac{V + IR_S}{R_P}\right)$$
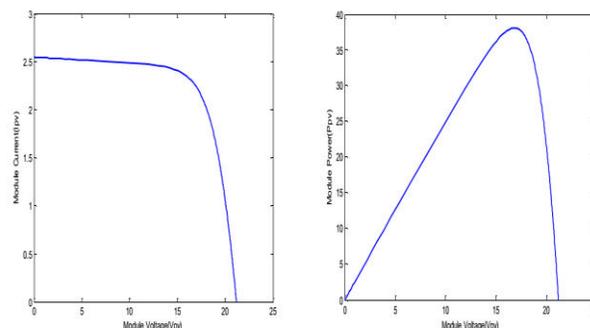
Where
I_{PV}–Photocurrent current,
I_O–diode's Reverse saturation current,
V–Voltage across the diode,
a– Ideality factor
V_T –Thermal voltage
R_s – Series resistance R_p –Shunt resistance

V-I & P-V Characteristics of a 36w PV module

A single-phase five-level photovoltaic (PV) inverter topology for grid-connected PV systems with a novel pulse width-modulated (PWM) control scheme. Two reference signals

International Journal for Innovative Engineering and Management Research
A Peer Reviewed Open Access International Journal
www.ijiemr.com

identical to each other with an offset equivalent to the amplitude of the triangular carrier signal were used to generate PWM signals for the switches. A digital proportional-integral current control algorithm is implemented in DSP TMS320F2812 to keep the current injected into the grid sinusoidal and to have high dynamic performance with rapidly changing atmospheric conditions. The inverter offers much less total harmonic distortion and can operate at near-unity power factor. The proposed system is verified through simulation and is implemented in a prototype, and the experimental results are compared with that with the conventional single-phase three-level grid-connected PWM inverter. They range from small residential and commercial rooftop systems to large utility-scale solar power stations. Unlike stand-alone power systems, a grid-connected system rarely includes an integrated battery solution, as they are still very expensive. When conditions are right, the grid-connected PV system supplies the excess power, beyond consumption by the connected load,

Residential, grid-connected rooftop systems which have a capacity more than 10 kilowatts can meet the load of most consumers.[2] They can feed excess power to the grid where it is consumed by other users. The feedback is done through a meter to monitor power transferred. Photovoltaic wattage may be less than average consumption, in which case the consumer will continue to purchase grid energy, but a lesser amount than previously. If photovoltaic wattage substantially exceeds average consumption, the energy produced by the panels will be much in excess of the demand. In this case, the excess power can yield revenue by selling it to the grid. Depending on their agreement with their local grid energy

company, the consumer only needs to pay the cost of electricity consumed less the value of electricity generated. This will be a negative number if more electricity is generated than consumed.[3] Additionally, in some cases, cash incentives are paid from the grid operator to the consumer.
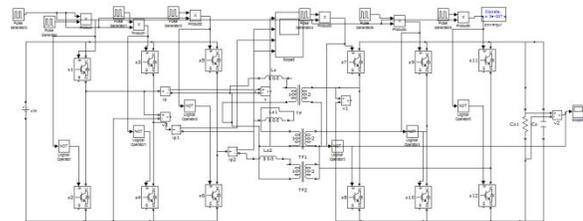
V.MATLAB/SIMULATION RESULTS

Fig 3 Matlab/simulation conventional circuit of three-phase DAB dc-dc converter Topology.
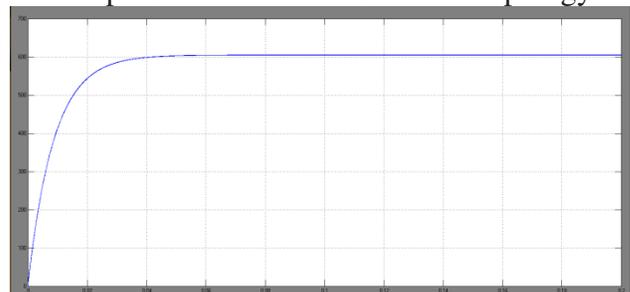

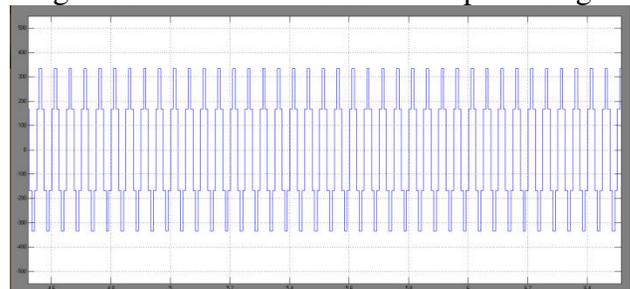Fig 4 simulation wave form of output voltage

Fig 5 simulation wave form of input line voltage at 750v
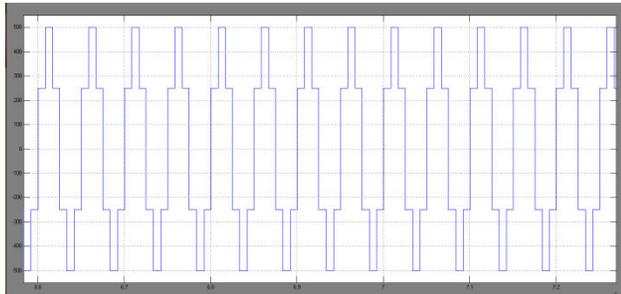
Fig 6 simulation wave form of input line voltage at 750 v
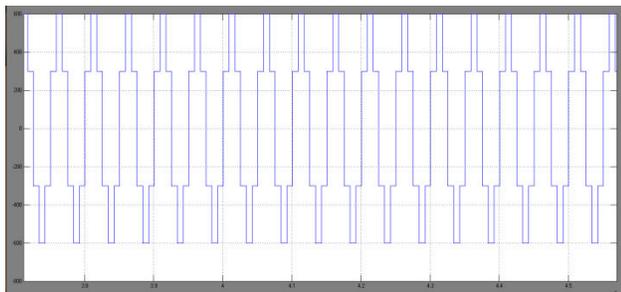

Fig 7 simulation wave form of input line voltage at 900v
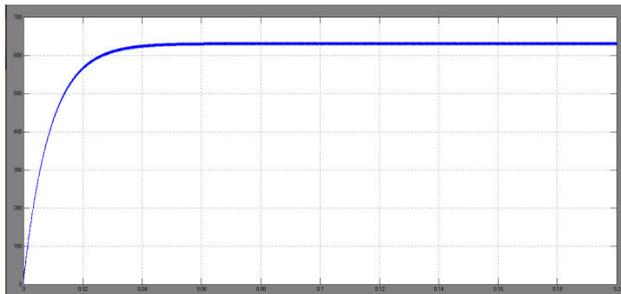

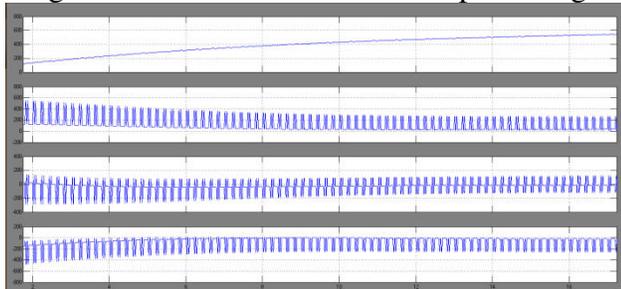Fig 8 simulation wave form of output voltage

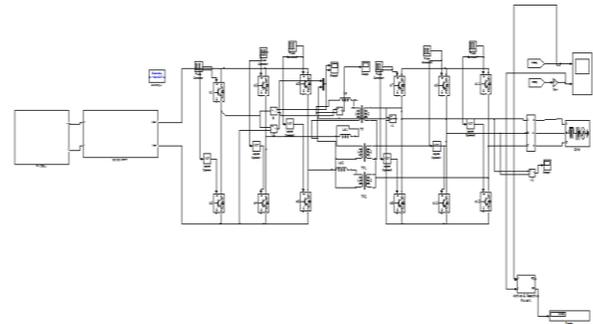Fig 9 simulation wave form of line voltages and currents

Fig 10 Matlab/simulation proposed method of three-phase DAB dc-dc converter Topology with PV and grid
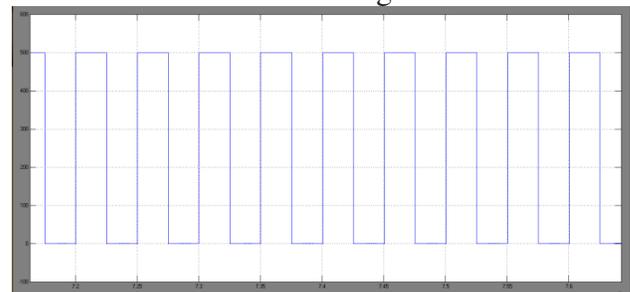

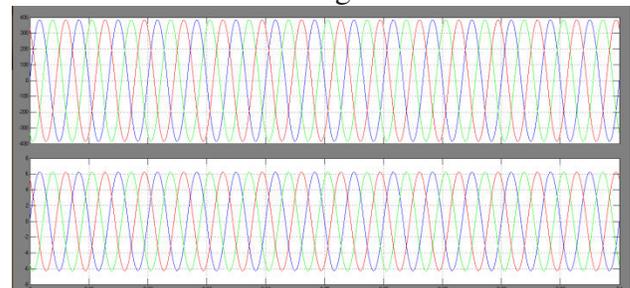Fig 11simulation wave form of dc-dc converter Topology with before grid connected output voltage

Fig 12 simulation wave form of dc-dc converter Topology with grid connected output voltage and current

VI.CONCLUSION

This work has evaluated the strategy for utilization of PV Cells for induction motor pumping. The electricity bill gets reduced since solar energy is utilized for agriculture pumping.

The Photo Voltaic powered three phase induction motor drive system is successfully designed, modeled and simulated using Matlab/Simulink. The concept of Photo Voltaic grid is proposed. The simulation results of three phase grid connected system for Photo Voltaic pumping are presented. The simulation results are in line with the theoretical results. The scope of this work is the simulation and implementation of three phases PV Powered grid connected system.

REFERENCES

[1].Nico H. Baars, Student Member, IEEE, Jordi Everts, Member, IEEE, Henk Huisman, Jorge L. Duarte, Member, IEEE, and Elena A. Lomonova, Senior Member, IEEE"A 80-kW Isolated DC–DC Converter m for Railway Applications"IEEE Transactions On Power Electronics, Vol. 30, No. 12, December 2015.

[2] R. De Doncker, D. Divan, and M. Kheraluwala, "A three-phase softswitched high-power-density dc/dc converter for high-power applications," IEEE Trans. Ind. Appl., vol. 27, no. 1, pp. 63–73, Jan. 1991.

[3] J. Dudrik, P. Spanik, and N.-D. Trip, "Zero-voltage and zero-current switching full-bridge dc-dc converter with auxiliary transformer," IEEE Trans. Power Electron., vol. 21, no. 5, pp. 1328–1335, Sep. 2006.

[4] J.-G. Cho, C.-Y. Jeong, and F. Lee, "Zero-voltage and zero-currentswitching full-bridge PWM converter using secondary active clamp," IEEE Trans. Power Electron., vol. 13, no. 4, pp. 601–607, Jul. 1998.

[5] O. Patterson and D. Divan, "Pseudo-resonant full bridge dc/dc converter," IEEE Trans. Power Electron., vol. 6, no. 4, pp. 671–678, Oct. 1991.

[6] R. Steigerwald, "A comparison of half-bridge resonant converter topologies," IEEE Trans. Power Electron., vol. 3, no. 2, pp. 174–182, Apr. 1988.

[7] A. Bhat and R. Zheng, "Analysis and design of a three-phase LCC-type resonant converter," IEEE Trans. Aerospace and Electron. Syst., vol. 34, no. 2, pp. 508–519, Apr. 1998.

[8] R. Steigerwald, "High-frequency resonant transistor dc-dc converters," IEEE Trans. Ind. Electron., vol. IE-31, no. 2, pp. 181–191, May 1984.

[9] X. Li, "A LLC-type dual-bridge resonant converter: Analysis, design, simulation, and experimental results," IEEE Trans. Power Electron., vol. 29, no. 8, pp. 4313–4321, Aug. 2014.

[10] J.-W. Kim and G.-W. Moon, "A new LLC series resonant converter with a narrow switching frequency variation and reduced conduction losses," IEEE Trans. Power Electron., vol. 29, no. 8, pp. 4278–4287, Aug. 2014.

[11] S. De Simone, C. Adragna, C. Spini, and G. Gattavari, "Design-oriented steady-state analysis of LLC resonant converters based on FHA," in Proc. Int. Symp. Power Electron., Electr. Drives, Autom. Motion,, May 2006, pp. 200–207.

[12] B.-C. Kim, K.-B. Park, C.-E. Kim, B.-H. Lee, and G.-W. Moon, "LLC resonant converter with adaptive link-voltage variation for a high-powerdensity adapter," IEEE Trans. Power Electron., vol. 25, no. 9, pp. 2248– 2252, Sep. 2010.

[13] Z. Hu, Y. Qiu, L. Wang, and Y.-F. Liu, "An interleaved LLC resonant converter operating at constant switching frequency," IEEE Trans. Power Electron., vol. 29, no. 6, pp. 2931–2943, Jun. 2014.

[14] M. Pavlovsky, S. de Haan, and J. Ferreira, "Reaching high power density in multikilowatt dc-dc converters with galvanic isolation," IEEE

Trans. Power Electron., vol. 24, no. 3, pp. 603–
612, Mar. 2009.